



# On-chip time resolved detection of quantum dot emission using integrated superconducting single photon detectors

G. Reithmaier<sup>1</sup>, S. Lichtmannecker<sup>1</sup>, T. Reichert<sup>1</sup>, P. Hasch<sup>1</sup>, K. Müller<sup>1</sup>, M. Bichler<sup>1</sup>, R. Gross<sup>2</sup> & J. J. Finley<sup>1</sup>

<sup>1</sup>Walter Schottky Institut, Physik Department and Center of Nanotechnology and Nanomaterials, Technische Universität München, 85748 Garching, Germany, <sup>2</sup>Walther-Meißner-Institut, Bayerische Akademie der Wissenschaften and Physik-Department, Technische Universität München, 85748 Garching, Germany.

We report the routing of quantum light emitted by self-assembled InGaAs quantum dots (QDs) into the optical modes of a GaAs ridge waveguide and its efficient detection on-chip via evanescent coupling to NbN superconducting nanowire single photon detectors (SSPDs). The waveguide coupled SSPDs primarily detect QD luminescence, with scattered photons from the excitation laser onto the proximal detector being negligible by comparison. The SSPD detection efficiency from the evanescently coupled waveguide modes is shown to be two orders of magnitude larger when compared with operation under normal incidence illumination, due to the much longer optical interaction length. Furthermore, in-situ time resolved measurements performed using the integrated detector show an average QD spontaneous emission lifetime of 0.95 ns, measured with a timing jitter of only 72 ps. The performance metrics of the SSPD integrated directly onto GaAs nano-photonic hardware confirms the strong potential for on-chip few-photon quantum optics using such semiconductor-superconductor hybrid systems.

Photonic information technologies using semiconductors are ubiquitous and are rapidly being pushed to the *quantum limit* where non-classical states of light can be generated and manipulated in nanoscale optical circuits<sup>1,2</sup>. Single photons can be readily generated on-chip<sup>3</sup> and preferentially routed into waveguide modes by carefully tailoring the local density of photonic modes experienced by the emitter<sup>4-6</sup>. Furthermore, *effective* interactions between photons can be induced by exploiting coherent light-matter couplings between the tightly localized vacuum field in nanoscale cavities, leading to remarkable phenomena such as *photon blockade*<sup>7,8</sup> needed for optical transistors<sup>9,10</sup> and ultrafast optical switching with only a few photons<sup>11</sup>. While the generation and routing of quantum light on a semiconductor chip<sup>3,12,13</sup> has already been demonstrated by several groups, the ability to generate *and* detect single photons on-chip with near unity quantum efficiency<sup>14</sup> and, moreover, integrate sources and detectors with nanophotonic hardware such as waveguides, high-Q nanocavities and beamsplitters would represent a major step towards the realization of semiconductor based quantum optical circuits.

In SSPDs, photon detection occurs via the formation of a normal conducting hotspot in a thin superconducting nanowire upon the absorption of a single photon<sup>15</sup>. Since the bias current flowing through the nanowire is slightly sub-critical ( $\sim 0.95 I_{crit}$ ), the local heating arising from single photon absorption results in the breakup of Cooper pairs, local switching of the nanowire to a normal conducting state and a measurable voltage pulse in the external readout circuit. Such SSPDs provide very high single photon detection efficiencies<sup>14,16-19</sup>, low dark count rates<sup>20</sup>, sensitivity from the visible to the IR<sup>21</sup> and picosecond timing resolution<sup>22,23</sup>. The possibility to integrate superconducting single photon detectors (SSPDs) onto dielectric<sup>14</sup> and plasmonic<sup>2</sup> waveguides results in a drastic increase of the absorption length for incoming photons, pushing the single-photon detection efficiency towards unity. Both the generation of cluster states of photonic qubits for one-way quantum computation<sup>24</sup> and the measurement based teleportation schemes<sup>25</sup> rely on having such near perfect detection efficiency.

Here, we demonstrate the on-chip generation of light originating from optically pumped micro-ensembles of  $\sim 100$  self-assembled InGaAs QDs, low loss guiding over  $\sim 0.5$  mm along a GaAs-AlGaAs ridge waveguide and high efficiency detection via evanescent coupling to an integrated SSPD. By comparing measurements performed with optical excitation above and below the GaAs bandgap, and exploring the temporal response of the system, we show that the detector signal overwhelmingly stems from QD luminescence with a negligible background from the laser. Power dependent measurements confirm the single photon sensitivity of the detectors and show that the

SUBJECT AREAS:  
PHOTONIC DEVICES  
QUANTUM DOTS  
SUPERCONDUCTING DEVICES  
QUANTUM OPTICS

Received  
12 March 2013

Accepted  
29 April 2013

Published  
28 May 2013

Correspondence and requests for materials should be addressed to G.R. (guenther.reithmaier@wsi.tum.de and finley@wsi.tum.de)

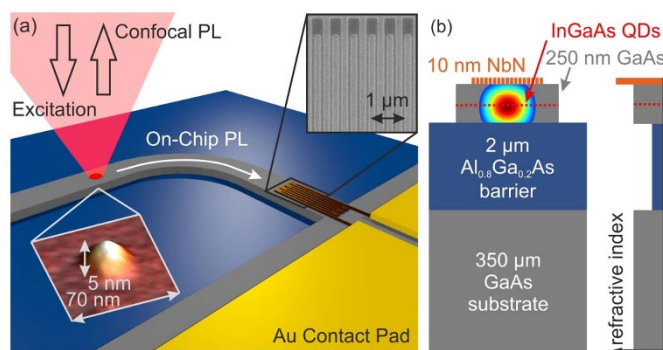


**Figure 1** | (a) Self assembled InGaAs quantum dots, as shown in the AFM image, embedded in a GaAs ridge waveguide are excited using a helium neon laser. The light emitted by the quantum dots is detected either in a confocal geometry or guided along the waveguide and evanescently coupled into a NbN superconducting nanowire single photon detector (SEM image in the inset). (b) Layer structure of the sample as prepared by molecular beam epitaxy and reactive magnetron sputtering. Refractive indices of the materials are schematically depicted on the rightmost side. A single layer of self-assembled InGaAs quantum dots is indicated by the dashed red line, overlapping with the maximum of the simulated intensity of the fundamental waveguide mode, shown in the contour plot.

SSPD is about two orders of magnitude *more sensitive* to waveguide photons than when illuminated in normal incidence. In-situ time resolved measurements performed using the integrated detector show an average QD spontaneous emission lifetime of  $0.95 \pm 0.03$  ns, with a low timing jitter of only  $72 \pm 2$  ps. The performance metrics of the SSPD integrated directly onto GaAs nano-photonic hardware confirms the strong potential for on-chip few-photon quantum optical experiments on a semiconductor platform<sup>2</sup>.

## Results

The samples investigated are composed of a GaAs multimodal ridge waveguide with a single layer of optically active self-assembled quantum dots, depicted schematically in figure 1a. An NbN superconducting single photon detector threads one end of the waveguide penetrating  $\sim 30 \mu\text{m}$  into the waveguide end. Figure 1b shows the sequence of the epitaxial layers and a vertical refractive index profile through the waveguide cladding, core and superconducting NbN nanowires. Detailed information concerning sample structure and preparation can be found in the methods section below. In order to estimate the maximum detection efficiency of such waveguide coupled SSPDs we simulated the optical field distribution of the fundamental waveguide mode using a commercial-grade eigenmode solver and propagator. The results obtained clearly show the maximum optical intensity close to the QD layer, as shown by the contour plot in figure 1b. Using the measured dielectric function of the NbN film ( $\epsilon = 3.5 + i 3.8$ ) we calculated that 97.8% of incident waveguide photons are absorbed by the detector, in good agreement with recent findings<sup>14,26</sup> for passive waveguide integrated SSPDs that revealed similarly high absorption. This near-unity value for the absorption probability should not be mistaken for the device detection efficiency, since the probability that an absorbed photon actually leads to a measurable voltage pulse has to be taken into account as well.

Spatially resolved photoluminescence (PL) measurements were performed whilst the sample was held at a nominal temperature of 4.2 K inside a cryogenic microwave probe station with optical access. This system provides a diffraction limited laser spot with a diameter of  $\sim 5 \mu\text{m}$  and allows the SSPD to be contacted using GHz voltage probes, thus, facilitating in-situ detection of PL routed along the waveguide. Data recorded using this measurement system is termed *on-chip PL* in the discussion below. For the operation conditions of the SSPD, as described in the methods section, the integrated

detector shows a negligible dark count rate  $< 10$  cps and a top-illumination detection efficiency of 0.001% for light at 940 nm, as expected for the relatively thick 10 nm NbN film<sup>21</sup>. This efficiency was estimated from the registered single photon events divided by the number of photons incident upon the active device area<sup>19</sup>. The active area of the device is given by the fractional areal coverage of NbN – 80 nm wide nanowires with a separation of 170 nm corresponding to a fill-factor of 32%. As discussed below, the detection efficiency for *waveguide photons* is about two orders of magnitude larger due to a significantly longer interaction length. Additional PL-spectroscopy measurements were performed on the same sample with excitation and detection normal to the waveguide axis using low temperature confocal microscope with a much higher spatial resolution ( $\sim 1 \mu\text{m}$ ). PL-spectra are obtained by dispersing the emitted light using a 0.5 m imaging monochromator and detected using a silicon CCD detector. In the following, such measurements are termed *confocal-PL*.

We begin by discussing *on-chip PL* recorded by raster scanning the excitation laser spot across the entire active waveguide structure. Typical results are presented in figure 2a that compares false color images of the SSPD count rate recorded using an excitation wavelength above the GaAs bandgap ( $\lambda = 632.8$  nm - red color coding) and selected regions of the device mapped with much longer wavelength excitation, far below the GaAs bandgap ( $\lambda = 940$  nm - blue color coding). All waveguide scans in figure 2a were recorded using the same excitation power density of  $25 \text{ W/cm}^2$ . At 940 nm, the excitation efficiency of the QDs is expected to be  $\sim 10^4 \times$  lower<sup>27</sup> whilst, as shown in the supplementary material, the reduction of the SSPD sensitivity is negligible ( $\sim 2.5 \times$ )<sup>21</sup>. Using above gap excitation the form of the waveguide can clearly be identified in the on-chip PL map in figure 2a, the count rate increasing significantly as the laser spot moves closer to the detector. In strong contrast, using 940 nm excitation only a background of  $\sim 1000$  cps is observed with no visible signal enhancement as the laser spot is scanned onto the waveguide. To systematically probe the wavelength selectivity we performed line scans across the remote waveguide end, farthest from the SSPD, along the line A-B marked in figure 2b. Line scans were made using non-resonant excitation above the GaAs bandgap (632.8 nm), below the GaAs bandgap into the wetting layer continuum (830 nm) and resonantly into the s-shell transitions of the QDs using far below bandgap excitation (940 nm). For above gap and wetting layer excitation, the waveguide can clearly be distinguished in the line scans. In contrast, with 940 nm excitation the waveguide topology could *not* be imaged (see figure 2b and figure 2a-inset) despite the detector remaining highly sensitive to such IR-illumination. This expectation is confirmed by the data presented in the inset of figure 2a that shows the direct normal incidence response of the detector at 940 nm when raster scanning the laser spot with a low power density of  $0.4 \text{ W/cm}^2$ . A clear maximum is observed when the laser spot is incident on the detector and, by measuring the normal incidence count rate and carefully calibrating the incident photon flux onto the detector, we estimated the top-illumination quantum efficiency to be  $\sim 0.001\%$  at 940 nm, in good accord with previous measurements<sup>19,21</sup> and expectations for a 10 nm thick NbN film. These observations clearly indicate that the signal detected when exciting on the waveguide arises from QD PL emitted into the waveguide mode and guided to the SSPD whereupon it is evanescently absorbed by the SSPD. This conclusion is unequivocally validated by the time-resolved measurements presented below.

For excitation at 632.8 nm close to the waveguide bend (figure 2a) using a power density of  $25 \text{ W/cm}^2$ , the typical maximum count rate on the detector ranged from 300 – 100 kcps when scanning the laser along the C – D marked line with a background count rate of  $< 10$  kcps recorded at position F, originating from scattered light on the sample surface. By exponentially fitting the intensity as a function of distance from the detector for the trajectories marked C – D and

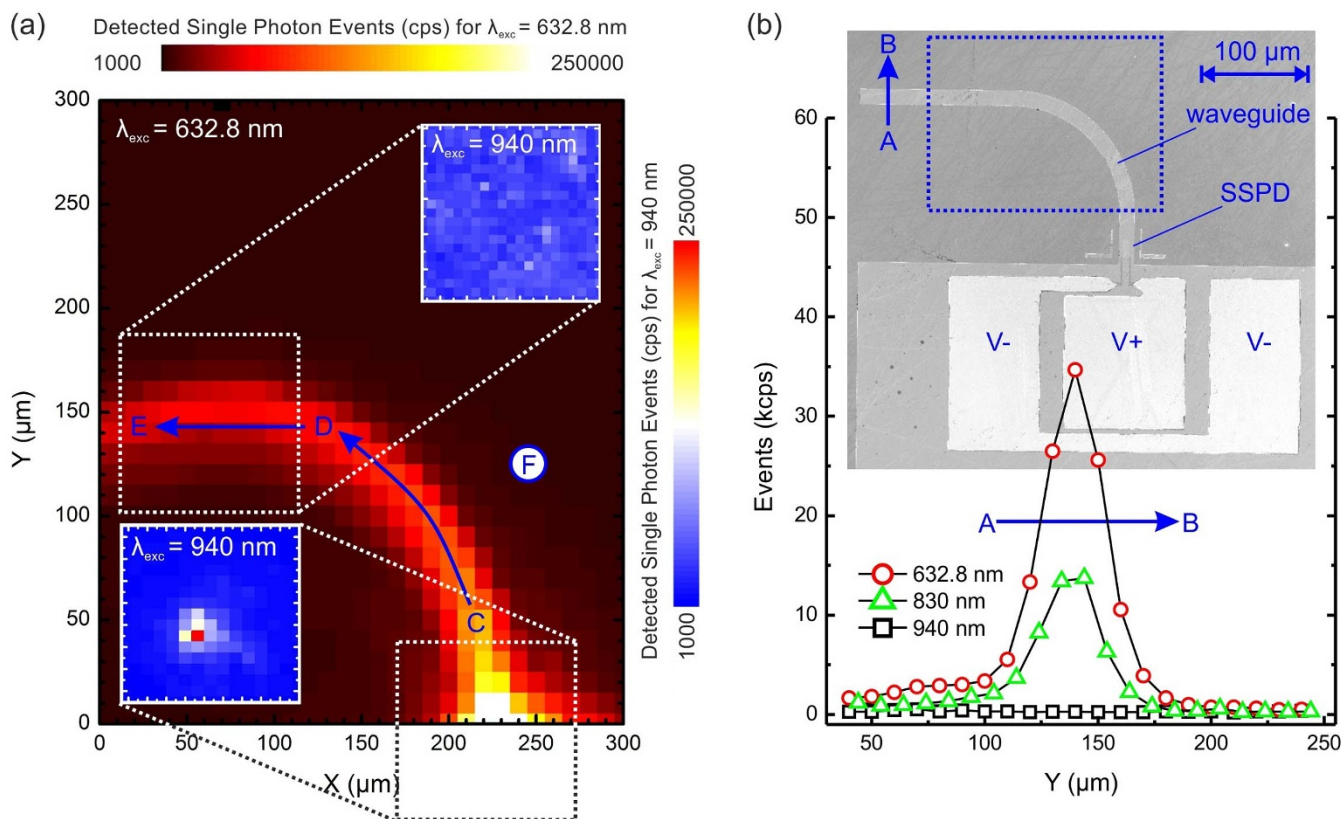


**Figure 2** | (a) Detected single photon events as a function of the laser position along the waveguide for  $\lambda_{\text{exc}} = 632.8$  nm, as shown in red color code. The two insets given with blue color code each correspond to a  $(100 \mu\text{m})^2$  area illuminated with  $\lambda_{\text{exc}} = 940$  nm. For illumination at the end of the waveguide only background light is detected, whereas a strong peak is observed at the position of the SSPD. (b) Recorded single photon events for line scans along the A-B marked line with different excitation wavelengths. The waveguide can clearly be identified for 632.8 nm and 830 nm, whereas only a small background is detected for 940 nm. The inset shows an SEM image of the analyzed structure with the scan area of figure 2a marked by a dotted line.

D – E, the waveguide losses are determined to be  $0.022 \text{ dB}/\mu\text{m}$  within the bend and  $0.005 \text{ dB}/\mu\text{m}$  in the straight segments, respectively (see supplementary material). Due to the low quantum dot density of  $\sim 6 \mu\text{m}^{-2}$ , reabsorption by quantum dots along the waveguide can be neglected<sup>28</sup>. As shown later in the discussion section, a lower limit for the SSPD detection efficiency for evanescently coupled quantum dot emission is estimated using these losses.

To unambiguously prove that the detected signal in in-situ PL measurements does indeed stem from QD emission, with a negligible laser background, we used the SSPD to perform time-resolved measurements. Here, the sample was excited using a 653 nm pulsed laser diode focused close to the remote waveguide end  $\sim 0.5$  mm from the SSPD. This source provided sub 60 ps duration pulses at a repetition rate of 20 MHz with low timing jitter  $< 3$  ps. The SSPD response was then read-out using a 20 GHz sampling oscilloscope to record a histogram of the time intervals between the trigger signal provided by the laser diode and the photon detection voltage pulse registered by the detector. Figure 3 shows typical time resolved data on a logarithmic scale including exponential fits to the rising and falling edge of the spontaneous emission dynamics. For comparison the instrument response function (IRF) of the detector and associated electronics was recorded using an IR pulsed laser source (952 nm,  $< 60$  ps pulse duration) focused directly onto the detector to avoid excitation of QD PL. Figure 3 shows the temporally sharp IRF from which a low timing jitter of  $72 \pm 2$  ps was obtained (figure 3 – inset)<sup>3</sup>. As jitters  $< 20$  ps have been reported<sup>22</sup> for similar SSPDs, in this case the jitter is most likely limited by the pulse duration of the laser. We fitted the rise ( $t_0$ ) and fall ( $t_1$ ) times of the observed on-chip PL time transient obtaining values of  $t_0 = 136 \pm 21$  ps and  $t_1 = 0.95 \pm 0.03$  ns, respectively. While  $t_1$  compares very well to the known

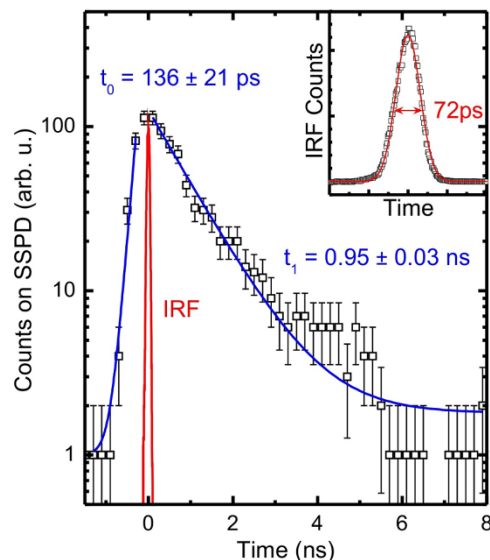


**Figure 3** | SSPD single photon events for ps - pulsed quantum dot excitation with 653 nm as a function of the photon arrival time shown as black squares. An exponential rise (decay) function given in blue reveals an average photon relaxation time (exciton lifetime) of  $136 \pm 21$  ps ( $0.95 \pm 0.03$  ns). The instrument response function showing a temporal resolution of 72 ps is given in red as well as in the inset.

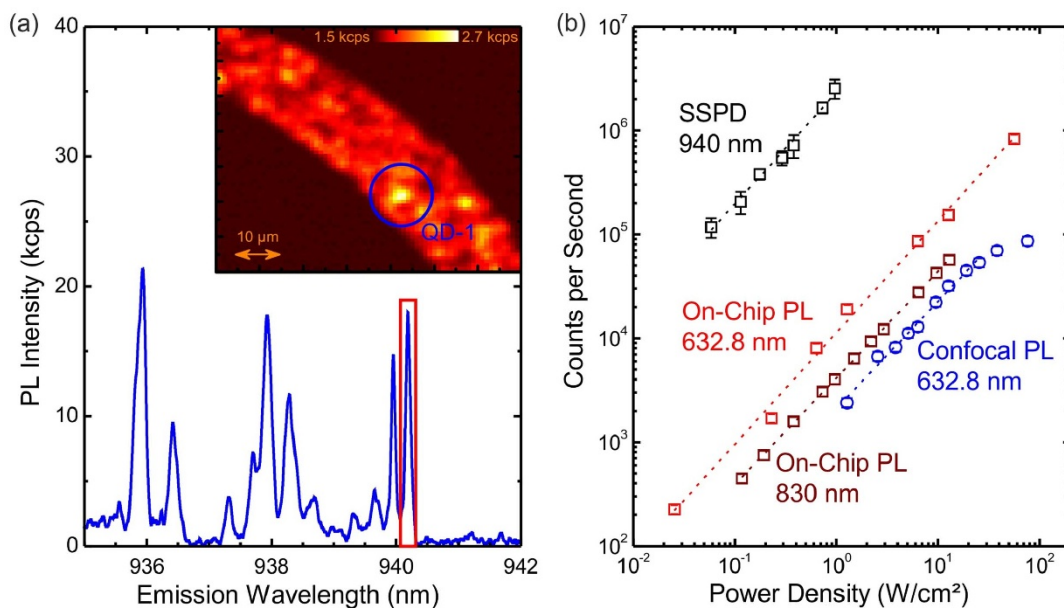


**Figure 4** | (a) Typical quantum dot luminescence spectrum for the position marked QD-1 in the inset. Inset: Spatially resolved quantum dot luminescence detected in confocal geometry for  $\lambda = 940.2 \pm 0.1$  nm (highlighted in red in the spectrum). (b) Detection events as a function of power density for direct SSPD illumination, as shown in black, and for quantum dot excitation, marked as “On-Chip PL”. For comparison the confocal PL of the exciton highlighted in figure 2a is shown in blue.

spontaneous emission lifetimes of InGaAs QDs<sup>4,5</sup>, the surprisingly slow rise-time reflects the timescale for carrier thermalization and capture into the dots from the surrounding GaAs, demonstrating the clear presence of a phonon bottleneck<sup>29</sup>. Evidently, the peak excitation power density provided by the pulsed excitation source ( $\sim 25$  W/cm<sup>2</sup>) is sufficiently low such as to keep the excitation regime firmly in the *single exciton* limit. In this case, significant free carrier populations are not present in the wetting layer and GaAs matrix that typically result in faster carrier capture and intra-dot carrier relaxation dynamics<sup>29</sup>. This expectation is supported by CW power dependent measurements presented below. Importantly, we note that a fast transient with the temporal profile of the excitation laser pulse is not observed close to  $t = 0$  ns in our time resolved measurements illustrating that the detected signal is dominated by QD PL and the SSPD signal does not contain scattered laser light.

## Discussion

Finally, we estimate a lower limit for the efficiency of our SSPD for evanescently coupled light by comparing the excitation power dependence of the QD-luminescence signal detected using *on-chip PL*, from  $\sim 120$  dots within the  $5 \mu\text{m}$  diameter laser focal volume<sup>30</sup> and *confocal-PL* from individual dots. A typical spectrum obtained using the confocal-PL geometry with excitation at 632.8 nm and a power density of  $6.4$  W/cm<sup>2</sup> is presented in figure 4a. Typically  $\sim 6$ – $20$  sharp lines are observed arising from different individual dots within the  $\sim 1 \mu\text{m}^2$  laser focal area. The inset in figure 4a shows the spatial distribution of the emission intensity within a  $0.1$  nm wide wavelength window centered on one such prominent single exciton transition, labeled QD-1 at 940.2 nm. The image clearly shows several localized emission centers arising from individual dots<sup>30</sup>. Figure 4b (blue circles) shows the power dependent intensity of QD-1 recorded using confocal-PL. A perfectly linear increase of the intensity is observed for excitation power densities  $< 10$  W/cm<sup>2</sup> confirming that the peak QD-1 arises from a single exciton transition from an individual dot<sup>31</sup>. As the excitation power increases to  $P_o \sim 55$  W/cm<sup>2</sup> the intensity of the single exciton saturates, and is then expected to decrease at higher power as the dot occupation shifts further into the multi-exciton regime. The maximum PL-intensity

arising from the neutral exciton transition corresponds to a time averaged exciton occupation probability in the dot of  $N_X \sim 1^{31}$ . The majority of the emission lines observed in figure 4a exhibit a similar power dependence indicating that, for the low excitation power densities used in figure 4a, they all stem from single exciton transitions from different dots addressed by the laser. Assuming that the number of randomly generated electron hole pairs inside a dot at any instant obeys Poisson statistics, an assumption that is likely to hold for excitation power densities  $P \ll P_o$ <sup>32</sup>, the probability that any dot is occupied with a single exciton is  $P_X = \alpha \times \exp(-P/P_o)$  where  $\alpha = P/P_o$  and the probability of  $n$ -excitons populating the dot is given by  $P_{nX} = \alpha^n \times \exp\left(-\frac{P}{P_o n!}\right)$ . For  $P \ll P_o$  the photon emission rate into the waveguide mode by a *single* pumped dot will, to a good approximation, be dominated by single excitons and, hence, is given by  $\phi \sim \frac{P_X(P)}{t_1} = \left(\frac{P}{P_o}\right) \exp(-P/P_o)/t_1$ , where  $t_1 = 0.95$  ns is the spontaneous emission lifetime determined above. Thus, for an excitation power density of  $\sim 10$  W/cm<sup>2</sup> ( $P/P_o \sim 0.2$ ,  $\exp(-P/P_o) = 0.82$ ), the maximum photon flux generated in the waveguide mode by dots within the laser focal volume is  $\phi_{max} \sim \left(\frac{P}{P_o}\right) \exp\left(-\frac{P}{P_o}\right) N_{QD} A_{laser} \zeta \eta / t_1$ , where  $N_{QD} \sim 6 \mu\text{m}^{-2}$  is the areal density of QDs,  $A_{laser}$  is the area of the laser spot,  $\zeta = -6.5$  dB  $\equiv 22\%$  accounts for the waveguide losses, as calculated in the discussion related to figure 2, and  $\eta = 6\%$  is the radiation fraction of the spontaneous emission into the waveguide mode, calculated by assuming each quantum dot is an ideal point dipole emitter. Using this information we are now in a position to estimate a lower limit for the SSPD detection probability. For on-chip PL we have  $A_{laser} = 20 \mu\text{m}^2$  from which we estimate that the maximum possible photon flux in the waveguide mode close to the SSPD to be  $\phi_{max} \sim (0.2 \times 0.82 \times 120 \times 0.22 \times 0.06) / (0.95) \text{ ns}^{-1}$  from which we would estimate a count rate of  $\sim 0.3 \pm 0.1 \times 10^9$  cps for the on-chip PL measurement with excitation at 632.8 nm with a power density of  $\sim 10$  W/cm<sup>2</sup> (red squares - figure 4b). The on-chip PL dataset as well as the SSPD counts for direct illumination (black



squares) clearly show a linear power dependence with an exponent of  $1.06 \pm 0.03$  reflecting single photon sensitivity of the detector<sup>6</sup>. Taking the measured count rates in on-chip PL into account and considering the experimentally determined waveguide losses and the simulated absorption of the detector, we estimate the detection efficiency of the 10 nm thick SSPD for evanescently coupled light to be  $\sim 0.1\%$ . The discrepancy between the simulated photon absorption of  $\sim 97.8\%$  and the measured device efficiency stems from the rather low probability that an absorbed photon leads to a detection event, as expected for a 10 nm thick detector<sup>19</sup>. Hence, this value could be improved significantly by using thinner NbN layers<sup>19,21</sup> for which near-unity quantum efficiency can be achieved in waveguide coupled detectors<sup>14</sup>. However, we note that the estimated detectivity of  $\sim 0.1\%$  is  $\sim 100 \times$  larger than that for normal incidence illumination.

In summary, we presented the creation, routing and detection of single quanta of light on a single chip. Using a waveguide coupled SSPD detector we showed that on-chip PL provides a detection efficiency of  $\sim 0.1\%$  for evanescently coupled light which gives a signal enhancement of two orders of magnitude when compared to top-illumination of the device. Moreover, it was shown that the integrated detector can be employed to perform in-situ time resolved measurements at a temporal resolution of 72 ps, thereby revealing an average exciton lifetime of  $0.95 \pm 0.03$  ns and a rise time of  $136 \pm 21$  ps. The great potential of this highly integrated quantum optics system can be fully used when additionally implementing the spectral resolution of SSPDs<sup>7</sup> or when performing resonant excitation experiments with single quantum dots.

## Methods

**Sample preparation.** The samples investigated were grown using solid source molecular beam epitaxy and consisted of a 350 nm thick GaAs buffer onto which a 2  $\mu\text{m}$  thick  $\text{Al}_{0.8}\text{Ga}_{0.2}\text{As}$  waveguide cladding layer was deposited. Following this, a 250 nm thick GaAs waveguide core was grown into which a layer of self-assembled InGaAs quantum dots was embedded at its midpoint. The growth conditions used resulted in dots with a typical lateral (vertical) size of  $25 \pm 5$  nm ( $5 \pm 1$  nm) as shown in the inset of figure 1a, an areal density of  $6 \pm 1 \mu\text{m}^{-2}$  and photoluminescence emission around  $\sim 920$  nm at 4 K with a FWHM of 60 nm. After growth, the native oxide was removed from the sample surface using an HCl dip and a high quality 10  $\pm$  0.5 nm thick NbN superconducting film was deposited using DC reactive magnetron sputtering. By carefully optimizing the deposition temperature, rate and the Nb:N ratio, high quality superconducting films were obtained on the GaAs substrate ( $T_C = 10.2 \pm 0.2$  K), despite the 26% lattice mismatch<sup>19,33,34</sup>. The complete layer sequence and refractive index profile of waveguide cladding, core and superconducting NbN nanowires is shown in figure 1b.

The nanowire detector was then defined using electron beam lithography with a negative tone resist and reactive ion etching using a  $\text{SF}_6/\text{C}_4\text{F}_8$  plasma to form an NbN nanowire meander consisting of  $34 \times 80 \pm 10$  nm wide nanowires separated by  $170 \pm 10$  nm to form a detector with a width of 8.5  $\mu\text{m}$  and a total length of 23  $\mu\text{m}$  along the waveguide axis. A scanning electron microscope image of the resulting NbN nanowires on GaAs is presented in figure 1a - inset. Subsequently  $\sim 500 \mu\text{m}$  long, 17  $\mu\text{m}$  wide multimodal ridge waveguides were defined using photolithography and wet etching in a citric acid +  $\text{H}_2\text{O}_2$  solution. The waveguides feature a  $90^\circ$  gradual bend at their midpoint having a radius of curvature of 150  $\mu\text{m}$  as depicted schematically in figure 1a. The waveguides were defined such that the nanowire detector is centered on one end, penetrating  $\sim 30 \mu\text{m}$  into the waveguide end to ensure optimum evanescent coupling<sup>14</sup>.

**Device operation and characterization.** The SSPD was operated at liquid helium temperatures inside a cryogenic microwave probe station. A bias-tee was used to drive a fixed bias current of  $I = 0.95 \times I_C = 6.0 \mu\text{A}$  through the nanowires<sup>19</sup>. A low noise voltage source in series with a 100 k $\Omega$  resistor was operated as a constant current source. Voltage pulses arising from single photon detection events were then amplified using two 30 dB high-bandwidth amplifiers and detected with a 350 MHz frequency counter. The time-resolved measurements presented in figure 3 were performed using a 20 GHz sampling oscilloscope to record histograms of the time intervals between the trigger signal provided by the ps-pulsed laser source and the voltage pulse arising upon photon detection.

- Politi, A., Matthews, J., Thompson, M. G. & O'Brien, J. L. Integrated quantum photonics. *IEEE J. Quantum Electron* **15**, 1673–1684 (2009).
- Matthews, J. C. F., Politi, A., Stefanov, A. & O'Brien, J. L. Manipulation of multiphoton entanglement in waveguide quantum circuits. *Nature Photon* **3**, 346–350 (2009).

- Laucht, A. *et al.* A waveguide-coupled on-chip single-photon source. *Phys. Rev. X* **2**, 011014 (2012).
- Viasnoff-Schwob, E. *et al.* Spontaneous emission enhancement of quantum dots in a photonic crystal wire. *Phys. Rev. Lett.* **95**, 183901 (2005).
- Manga Rao, V. S. C. & Hughes, S. Single quantum dot spontaneous emission in a finite-size photonic crystal waveguide: proposal for an efficient “on chip” single photon gun. *Phys. Rev. Lett.* **99**, 193901 (2007).
- Thyrrstrup, H., Sapienza, L. & Lodahl, P. Extraction of the  $\beta$ -factor for single quantum dots coupled to a photonic crystal waveguide. *Appl. Phys. Lett.* **96**, 231106 (2010).
- Birnbaum, K. M. *et al.* Photon blockade in an optical cavity with one trapped atom. *Nature* **436**, 87–90 (2005).
- Reinhard, A. *et al.* Strongly correlated photons on a chip. *Nature Photon* **6**, 93–96 (2012).
- Chang, D. E., Sørensen, A. S., Demler, E. A. & Lukin, M. A single-photon transistor using nanoscale surface plasmons. *Nature Phys.* **3**, 807–812 (2007).
- Hwang, J. *et al.* A single-molecule optical transistor. *Nature* **460**, 76–80 (2009).
- Volz, T. *et al.* Ultrafast all-optical switching by single photons. *Nature Photon* **6**, 605–609 (2012).
- Schwagmann, A. *et al.* On-chip single photon emission from an integrated semiconductor quantum dot into a photonic crystal waveguide. *Appl. Phys. Lett.* **99**, 261108 (2011).
- Hoang, T. B. *et al.* Enhanced spontaneous emission from quantum dots in short photonic crystal waveguides. *Appl. Phys. Lett.* **100**, 061122 (2012).
- Pernice, W. *et al.* High-speed and high-efficiency travelling wave single-photon detectors embedded in nanophotonic circuits. *Nature Comm.* **3**, 1325 (2012).
- Skocpol, W. J., Beasley, M. R. & Tinkham, M. J. Self-heating hotspots in superconducting thin-film microbridges. *Appl. Phys.* **45**, 4054 (1974).
- Marsili, F. *et al.* High efficiency NbN nanowire superconducting single photon detectors fabricated on MgO substrates from a low temperature process. *Optics Express* **16**, 3191–3196 (2008).
- Hu, X. *et al.* Fiber-coupled nanowire photon counter at 1550 nm with 24% system detection efficiency. *Optics letters* **34**, 3607–3609 (2009).
- Kerman, A. J. *et al.* Constriction-limited detection efficiency of superconducting nanowire single-photon detectors. *Appl. Phys. Lett.* **90**, 101110 (2007).
- Reithmaier, G. *et al.* Optimisation of NbN thin films on GaAs substrates for in-situ single photon detection in structured photonic devices. *J. Appl. Phys.* **113**, 143507 (2013).
- Kitaygorsky, J. *et al.* Dark Counts in Nanostructured NbN Superconducting Single-Photon Detectors and Bridges. *IEEE Trans. Appl. Supercond* **17**, 275–278 (2007).
- Hofherr, M. *et al.* Intrinsic detection efficiency of superconducting nanowire single-photon detectors with different thicknesses. *J. Appl. Phys.* **8**, 014507 (2010).
- Gol'tsman, G. N. *et al.* Ultrafast superconducting single-photon detectors for near-infrared-wavelength quantum communications. *Phys. Stat. Sol. C* **2**, 1480–1488 (2005).
- Najafi, F., Marsili, F., Dauler, E., Molnar, R. J. & Berggren, K. K. Timing performance of 30-nm-wide superconducting nanowire avalanche photodetectors. *Appl. Phys. Lett.* **100**, 152602 (2012).
- Walther, P. *et al.* Experimental one-way quantum computing. *Nature* **434**, 169–176 (2005).
- Knill, E., Laflamme, R. & Milburn, G. J. A scheme for efficient quantum computation with linear optics. *Nature* **409**, 46–52 (2001).
- Sprengers, J. P. *et al.* Waveguide superconducting single-photon detectors for integrated quantum photonic circuits. *Appl. Phys. Lett.* **99**, 18110 (2011).
- Fry, P. W. *et al.* Photocurrent spectroscopy of InAs/GaAs self-assembled quantum dots. *Phys. Rev. B* **24**, 16784 (2000).
- Herrmann, E., Smowton, P. M., Summers, H. D., Thomson, J. D. & Hopkinson, M. Modal gain and internal optical mode loss of a quantum dot laser. *Appl. Phys. Lett.* **77**, 163–166 (2000).
- Urayama, J., Norris, T. B., Singh, J. & Bhattacharya, P. Observation of Phonon Bottleneck in Quantum Dot Electronic Relaxation. *Phys. Rev. Lett.* **86**, 4930–4933 (2001).
- A careful analysis of the number of detected emission centers recorded by exciting the imaging the dot emission directly onto a silicon CCD imager reveals a dot density of  $6 \pm 1/\mu\text{m}^2$ .
- Finley, J. J. *et al.* Charged and neutral exciton complexes in individual self-assembled In(Ga)As quantum dots. *Phys. Rev. B* **63**, 073307 (2001).
- Bacher, G. *et al.* *Phys. Rev. Lett.* **83**, 4417 (1999) and references therein.
- Gaggero, A. *et al.* Nanowire superconducting single-photon detectors on GaAs for integrated quantum photonic applications. *Appl. Phys. Lett.* **97**, 151108 (2010).
- Marsili, F. *et al.* High quality superconducting NbN thin films on GaAs. *Supercond. Sci. Tech.* **22**, 095013 (2009).

## Acknowledgements

We gratefully acknowledge D. Sahin, A. Fiore (TU Eindhoven) and K. Berggren, F. Najafi (MIT) and R. Hadfield (Heriot-Watt) and M. C. Amann (TUM) for useful discussions and the BMBF for financial support via QuaHL-Rep Project number 16BQ1036, the EU via the integrated project SOLID and the DFG via SFB 631-B3 and Nanosystems Initiative Munich.



### Author contributions

G.R., S.L., P.H. and J.J.F. conceived and designed the experiments. G.R. and P.H. prepared the samples and performed the experiments. G.R., S.L. and P.H. analyzed the data. K.M., T.R., M.B. and R.G. contributed materials/analysis tools. G.R. and J.J.F. wrote the paper. All authors reviewed the manuscript.

### Additional information

Supplementary information accompanies this paper at <http://www.nature.com/scientificreports>

**Competing financial interests:** The authors declare no competing financial interests.

**License:** This work is licensed under a Creative Commons Attribution-NonCommercial-NoDerivs 3.0 Unported License. To view a copy of this license, visit <http://creativecommons.org/licenses/by-nc-nd/3.0/>

**How to cite this article:** Reithmaier, G. *et al.* On-chip time resolved detection of quantum dot emission using integrated superconducting single photon detectors. *Sci. Rep.* 3, 1901; DOI:10.1038/srep01901 (2013).